

# Performance of Bi–Te–Sb–Se Thermoelectric Material at Low Temperature<sup>1</sup>

Lei Jia,<sup>2</sup> Peng Hu,<sup>2</sup> Zeshao Chen,<sup>2,3</sup> and Wei Sun<sup>2</sup>

---

Thermoelectric materials are of interest for applications as heat pump and power generators. The performance of a thermoelectric material, the figure of merit,  $ZT$ , is measured. The figure of merit is interrelated to the thermal conductivity, electrical conductivity, and Seebeck coefficient. All of these parameters are functions of temperature. The performance of a Bi–Te–Sb–Se thermoelectric material at low temperature was studied experimentally in this work. Based on the experimental results, the relation between various parameters and temperature, and the figure of merit are reported. The conclusions indicate that this thermoelectric material is not suitable for power generation at low temperature, and only an improvement of production technology or the development of a new production method can improve the electrical power generation performance with this method.

---

**KEY WORDS:** electrical conductivity; low temperature; Seebeck coefficient; thermal conductivity; thermoelectric.

## 1. INTRODUCTION

Thermoelectric (TE) generators are unconventional power sources that are being researched vigorously. From the first discovery of the Seebeck effect in 1821 and up to the 1950s, the technology of thermoelectric generation was primitive. There were not any suitable materials available, and most usage of the thermoelectric effect involved the well known thermocouple. Since the 1950s, the development of production technology using excellent

---

<sup>1</sup> Paper presented at the Seventh Asian Thermophysical Properties Conference, August 23–28, 2004, Hefei and Huangshan, Anhui, P. R. China.

<sup>2</sup> Department of Thermal Science and Energy Engineering, University of Science and Technology of China, Hefei 230027, P. R. China.

<sup>3</sup> To whom correspondence should be addressed. E-mail: zschen@ustc.edu.cn

semiconductors has been extremely rapid. Semiconductor materials with low thermal conductivity, good electrical conductivity, and a large Seebeck coefficient have been used in thermoelectric devices to produce electrical power. This is because of their small size, simplicity, quietness, and reliability. Yamanaka et al. [1] evaluated the thermoelectric properties of layered rare earth copper oxides. Khitun et al. [2] investigated methods to enhance the thermoelectric figure of merit in a quantum dot superlattice. The first experimental observation of a very large enhancement of the thermoelectric power of composites containing bismuth nanowires with diameters of 9 and 15 nm has been reported [3].

At present, research on thermoelectric power generation applications focuses mostly on the utilization of low-grade thermal energy, such as geothermal energy, solar energy, and ocean energy, which are utilized at temperatures above ambient. However, energy at low temperatures can also be useful, and can be used for thermoelectric power generation. For example, liquefied natural gas (LNG) is clean energy and is heated from 112 K to room temperature for use, and the energy for heating is about  $900 \text{ kJ}\cdot\text{kg}^{-1}$ . It is obvious that there is plenty of cold energy that can be utilized during the heating process.

Cold energy can be directly converted into electrical power by thermoelectric generators. Most thermoelectric generators are made of semiconductor arms and river diversion metal. The performance of thermoelectric generators is mainly determined by the performance of thermoelectric materials. Some alloys composed of Bi, Te, Sb, and Se are suitable thermoelectric materials at low temperature. Three parameters influencing the thermoelectric materials are the thermal conductivity, electrical conductivity, and Seebeck coefficient which are interrelated. The performance of thermoelectric materials depends on the figure of merit ( $ZT$ ), given by

$$ZT = \frac{S^2\sigma}{\lambda}T \quad (1)$$

where  $S$ ,  $\sigma$ ,  $\lambda$ , and  $T$  are the Seebeck coefficient, electrical conductivity, thermal conductivity and absolute temperature, respectively.

A high  $ZT$  appears to be about 1.14 for a  $p$ -type  $(\text{Bi}_2\text{Te}_3)_{0.25}(\text{Sb}_2\text{Te}_3)_{0.72}(\text{Sb}_2\text{Se}_3)_{0.03}$  alloy [4]. A textured  $p$ -type  $(\text{Bi,Sb})_2\text{Te}_3$  reaches the highest  $ZT$  of 1.15 [5]. The synthesis and thermoelectric properties of  $\text{Bi}_2\text{Te}_3$ -based nanocomposites have been investigated, and its maximal  $ZT$  value is 0.83 [6]. A  $ZT$  value greater than one in crystals of Bi–Sb alloy under a magnetic field at about 100 K has been reported [7].  $\text{CsBi}_4\text{Te}_6$  is another high performance thermoelectric material below room temperature, and its  $ZT$  is about 0.8 at 225 K, which appears to match those of Bi–Te–Sb–Se alloys [8]. There is no apparent thermodynamic upper limit

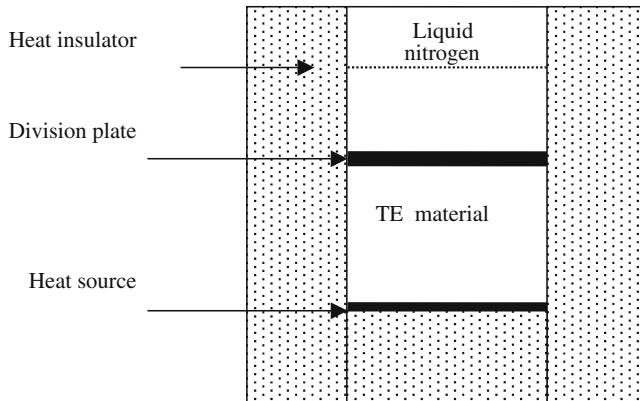


Fig. 1. Schematic of test system for thermal conductivity measurements of semiconductor.

on  $ZT$ ; in addition to its engineering importance, values of  $ZT$  significantly larger than unity are of interest to transport theory [9].

The semiconductors investigated in this paper are

$p$  - type : 74 mol%  $\text{Sb}_2\text{Te}_3$  + 26 mol%  $\text{Bi}_2\text{Te}_3$  + impurity;

$n$  - type : 93 mol%  $\text{Bi}_2\text{Te}_3$  + 7 mol%  $\text{Bi}_2\text{Se}_3$  + impurity.

## 2. MEASUREMENTS

### 2.1. Thermal Conductivity

The thermal conductivity of thermoelectric materials was measured by a static method, as shown in Fig. 1. The heat source was made of Minalpha, and the thermoelectric material was placed on the heat source. Liquid nitrogen was used and was placed above the semiconductor. Between the thermoelectric material and liquid nitrogen, there was a division plate with different thicknesses, which not only protects the thermoelectric materials but also helps to equilibrate the cold side temperature. Thermocouples were placed on the upper and lower surfaces of the TE material in order to measure the temperature of cold and hot sides. The acquisition instrument was HP34970A, and the uncertainty in the current was at the mA level. During the experiments, the temperature difference  $\Delta T$  between the hot and cold sides was about 6 K. The thermal conductivity is given by

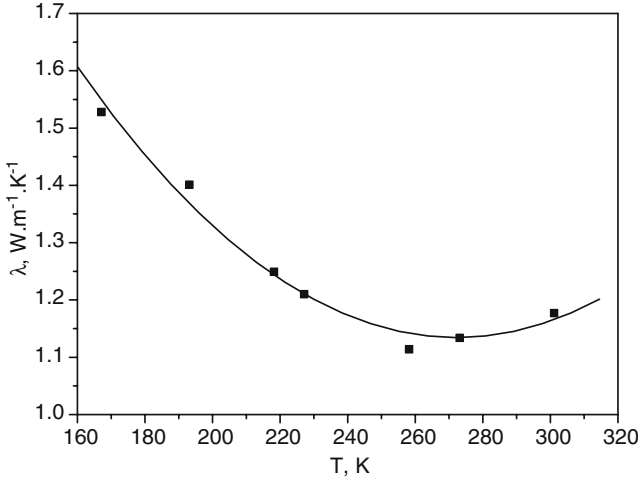


Fig. 2. Thermal conductivity of *n*-type semiconductor as a function of temperature.

$$\lambda = \frac{I^2 RL}{A \Delta T} \quad (2)$$

where  $I$ ,  $R$ ,  $L$ , and  $A$  are the current, the electrical resistance of the heat source, the length of TE material, and the cross-sectional area of TE material, respectively.

The main experimental errors came from measurements of the temperature difference. Because the thermocouples directly contacted the specimen, thermocouples with small diameters and low thermoelectric conductivity should be used to minimize the errors. In this study, the temperature difference was measured twice and the mean was used in Eq. (2).

The thermal conductivity of *n*-type and *p*-type semiconductor TE materials was measured, as shown in Figs. 2 and 3, respectively. The black dots are experimental results. It is seen clearly from Figs. 2 and 3 that a minimum in thermal conductivity appears at about 260–270 K, for both *n*-type and *p*-type semiconductors. The thermal conductivity of any material is composed of two parts: the electron thermal conductivity and phonon thermal conductivity. For a semiconductor, the contribution of the electron thermal conductivity is very small. The phonon thermal conductivity dramatically increases with decreasing temperature at relatively low temperature, which is disadvantageous for electrical power generation.

Based on the fitted experimental results, the thermal conductivity as a function of absolute temperature is given by

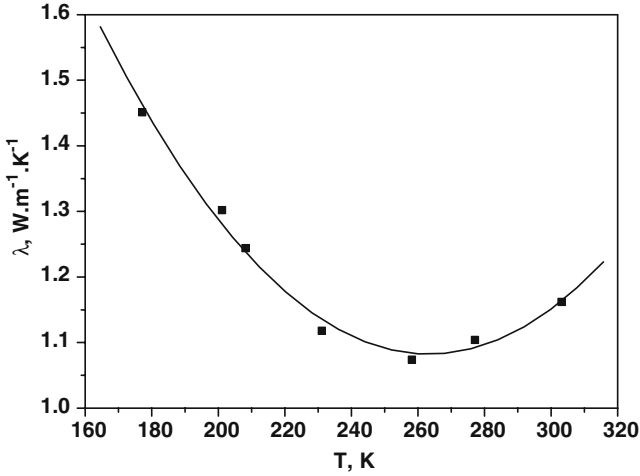


Fig. 3. Thermal conductivity of *p*-type semiconductor as a function of temperature.

$$n\text{-type: } \lambda_N = 3.91017 - 0.02039T + 3.74568 \times 10^{-5}T^2 \quad (\text{W} \cdot \text{m}^{-1} \cdot \text{K}^{-1}) \quad (3)$$

$$p\text{-type: } \lambda_P = 4.63215 - 0.02696T + 5.12003 \times 10^{-5}T^2 \quad (\text{W} \cdot \text{m}^{-1} \cdot \text{K}^{-1}) \quad (4)$$

## 2.2. Electrical Conductivity

The electrical conductivity of TE materials was measured by the twin-probe method. The semiconductors are in the shape of a rectangular solid, with contact points for measurements of the current  $I$  and voltage  $U$  on both ends. The electrical conductivity is given by

$$\sigma = \frac{IL}{UA} \quad (5)$$

where  $L$  and  $A$  are the length and cross-sectional area of the TE material, respectively.

The electrical conductivity of *n*-type and *p*-type semiconductor TE materials were measured, as shown in Figs. 4 and 5. It is seen clearly from Figs. 4 and 5 that these TE materials show a certain metallic character for both *n*-type and *p*-type semiconductors. For example, the electrical conductivity of an *n*-type material is about  $400 \Omega^{-1} \cdot \text{cm}^{-1}$  at 280 K; however, it increases to about  $1500 \Omega^{-1} \cdot \text{cm}^{-1}$  at 100 K. The electrical conductivity

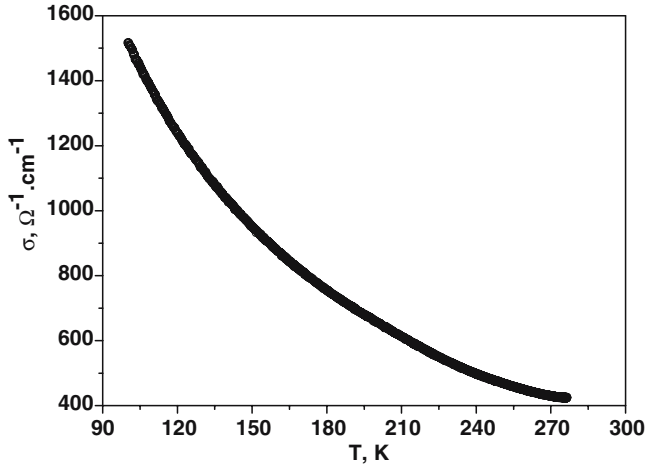


Fig. 4. Electrical conductivity of *n*-type semiconductor as a function of temperature.

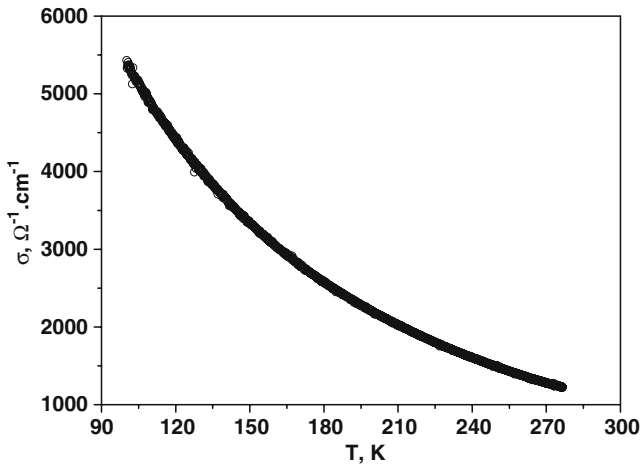


Fig. 5. Electrical conductivity of *p*-type semiconductor as a function of temperature.

of a *p*-type material is about  $1200 \Omega^{-1}\cdot\text{cm}^{-1}$  at 280 K: however, it reaches about  $5500, \Omega^{-1}\cdot\text{cm}^{-1}$  at 100 K. The range is very large, which is advantageous for electrical power generation at low temperature.

Based on the experimental results, the electrical conductivity as a function of absolute temperature is given by

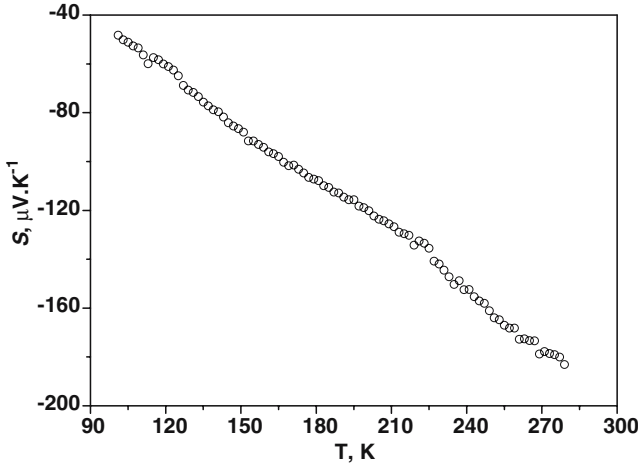


Fig. 6. Seebeck coefficient of  $n$ -type semiconductor as a function of temperature.

$$n\text{-type: } \sigma_N = 3584.876 - 29.424T + 0.097T^2 - 1.145 \times 10^{-4}T^3 (\Omega^{-1} \cdot \text{cm}^{-1}) \quad (6)$$

$$p\text{-type: } \sigma_P = 13305.254 - 112.837T + 0.381T^2 - 4.734 \times 10^{-4}T^3 (\Omega^{-1} \cdot \text{cm}^{-1}) \quad (7)$$

### 2.3. Seebeck Coefficient

The Seebeck coefficient of TE materials was measured by a static method, with a temperature difference  $\Delta T$  of about 2 K. The Seebeck coefficient is given by

$$S = \frac{E}{\Delta T} \quad (8)$$

where  $E$  is the electromotive force generated by  $\Delta T$ .

The Seebeck coefficients of  $n$ -type and  $p$ -type semiconductor TE materials were measured, and the results are shown in Figs. 6 and 7. It is seen clearly from Figs. 6 and 7 that the absolute values of the Seebeck coefficient of these TE materials dramatically decrease with the decreasing temperature at low temperature, for both  $n$ -type and  $p$ -type materials. For instance, the Seebeck coefficient of a  $n$ -type material is about  $-1.8 \times 10^{-4} \text{ V} \cdot \text{K}^{-1}$  at 280 K, and decreases to about  $-0.5 \times 10^{-4} \text{ V} \cdot \text{K}^{-1}$  at 100 K; the Seebeck coefficient of a  $p$ -type material is about  $1.4 \times 10^{-4} \text{ V} \cdot \text{K}^{-1}$  at

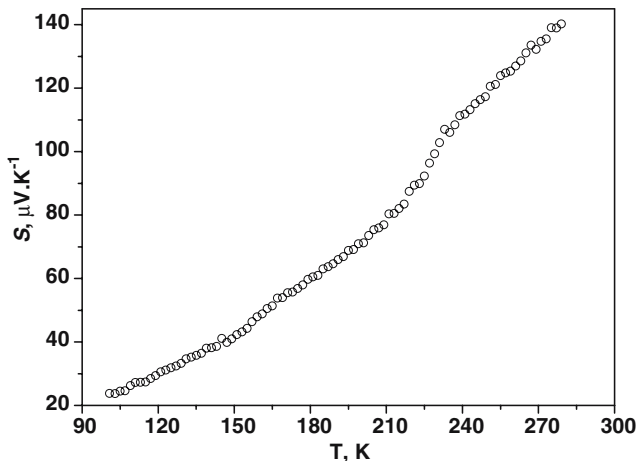


Fig. 7. Seebeck coefficient of  $p$ -type semiconductor as a function of temperature.

280 K, and decreases to about  $0.2 \times 10^{-4} \text{ V} \cdot \text{K}^{-1}$  at 100 K. The tendency is clear, which is disadvantageous for electrical power generation at low temperature.

Based on the fitted experimental results, the Seebeck coefficient as a function of absolute temperature is given by

$$n\text{-type: } S_N = 17.032 - 0.634T - 3.015 \times 10^{-4}T^2 \quad (\mu\text{V} \cdot \text{K}^{-1}) \quad (9)$$

$$p\text{-type: } S_P = 17.707 - 0.174T + 2.27 \times 10^{-3}T^2 \quad (\mu\text{V} \cdot \text{K}^{-1}) \quad (10)$$

#### 2.4. Influence of Thomson Effect on the Maximum Power Output

If a thermoelectric generator is composed of the materials discussed in this paper, the power output is given by [10]

$$P = (\alpha^h T^h - \alpha^c T^c)I - \tau \Delta T I - RI^2 \quad (11)$$

where  $\alpha^h$  and  $\alpha^c$  are the Seebeck coefficients of a generator at high temperature,  $T^h$ , and low temperature,  $T^c$ , respectively.  $I$  is the current, and  $\tau$  is the Thomson coefficient of the generator.  $R$  is the electrical resistance of the generator, and  $\Delta T = T^h - T^c$ .

When the load resistance  $R_L = R$ , the power output attains its maximum  $P_{\max}$ ,

$$P_{\max} = \frac{1}{4R} \left[ \alpha^h T^h - \alpha^c T^c - \tau \Delta T \right]^2 \quad (12)$$



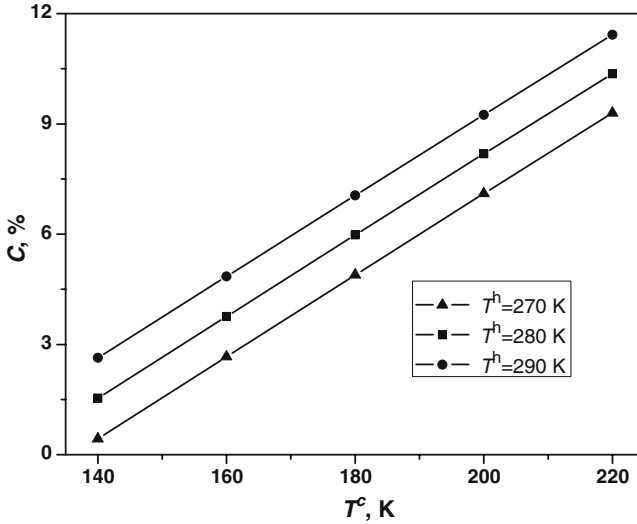


Fig. 8. Relationship between  $C$  and  $T^c$ .

The constant  $C$  is the ratio of the Thomson heat and  $P_{\max}$  when  $R_L = R$ ;

$$C = \frac{2\tau \Delta T}{\alpha^h T^h - \alpha^c T^c - \tau \Delta T} \quad (13)$$

For the materials investigated in this paper, the relation between  $C$  and  $T^c$  is shown in Fig. 8. From Fig. 8, it is clearly seen that the influence of the Thomson effect on the maximum power output decreases with decreasing  $T^c$ . The higher  $T^h$  is, the larger the influence is. It is obvious from Figs. 6 and 7 that the relationship between the Seebeck coefficient and temperature is approximately linear, and according to the definition of the Thomson coefficient  $\tau = T dS \cdot dT$ ,  $\tau$  will decrease with a decreasing working temperature. Another tendency shown in Fig. 8 is that if  $T^c$  is constant,  $C$  increases with increasing  $T^h$ . This is mainly dependent on increasing the working temperature and  $\tau$ .

The low temperature working range of LNG is about 140–170 K and the high temperature range is about 270–290 K.  $C$  is less than 5% within these ranges. The influence of the Thomson effect on the maximum power output can be ignored if the generator is composed of materials investigated in this paper. If the working temperature range varies, these parameters of the thermoelectric materials should be

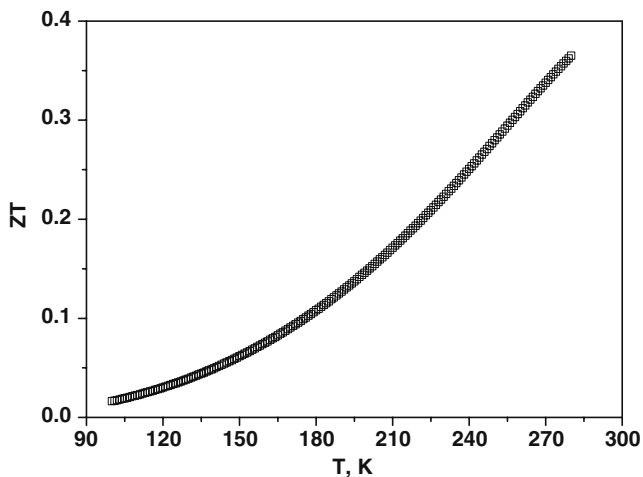


Fig. 9. Figure of merit of *n*-type semiconductor as a function of temperature.

reinvestigated and the influence of the Thomson effect should be discussed again.

## 2.5. Figure of Merit

The thermal conductivity, electrical conductivity and Seebeck coefficient are very important parameters for TE power generation, and the figure of merit is a critical parameter to judge the access of electrical power generation. All of these parameters are functions of absolute temperature. Substituting the functions above into Eq. (1), the curves of the figure of merit are generated, as shown in Figs. 9 and 10. It is obvious that the figure of merit of these materials decreases dramatically with decreasing absolute temperature.

## 2.6. Uncertainties

In thermal conductivity and electrical conductivity measurement systems, the uncertainty of  $I$ ,  $R$ ,  $L$ ,  $U$ , and  $\Delta T$  are 0.1 mA, 0.1  $\Omega$ , 0.1 mm, 0.1  $\mu$ V, and 0.1 K, respectively. In the Seebeck coefficient measurement system, the uncertainties of  $E$  and  $\Delta T$  are 0.1  $\mu$ V and 0.01 K, respectively. The maximum relative deviations of thermal conductivity, electrical conductivity and Seebeck coefficient are 1.1, 1.0, and 0.8%, respectively. Major errors come from the measurements of  $L$ ,  $R$ , and  $E$ . According to Eq. (1), the largest relative deviation of the figure of merit is 2.2%.

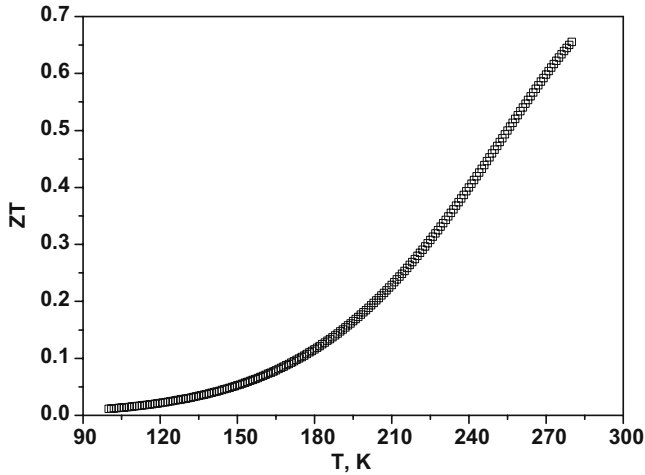


Fig. 10. Figure of merit of  $p$ -type semiconductor as a function of temperature.

### 3. CONCLUSION

Because of the relatively poor thermal conductivity and Seebeck coefficient properties, these TE materials are unsuitable for electrical power generation at low temperature. Improvement in product formulation can change the curves of figure of merit, and the development of new production methods, such as thin-film technology [11], can improve the power generation performance.

### ACKNOWLEDGMENTS

This work is supported by the State Research and Development Program of High Technology of China (Grant No. 2002AA515010).

### REFERENCES

1. S. Yamanaka, H. Kobayashi, and K. Kurosaki, *J. Alloys Compd.* **349**:321 (2003).
2. A. Khitun, K. L. Wang, and G. Chen, *Nanotechnology* **11**:327 (2000).
3. J. P. Heremans, C. M. Thrush, D. T. Morelli, and M. C. Wu, *Phys Rev Lett.* **88**:216801 (2002).
4. M. H. Ettenberg, W. A. Jesser, and F. D. Rosi, *Proc. 15th Int. Conf. on Thermoelectrics* (IEEE, Piscataway, NJ, 1996), pp. 52–56.
5. J. Jiang, L. D. Chen, S. Q. Bai, Q. Yao, and Q. Wang, *Scripta Materialia* **52**:347(2005).
6. H. L. Ni, X. B. Zhao, T. J. Zhu, X. H. Ji, and J. P. Tu, *J. Alloys Compd.* **397**:317(2005).

7. W. M. Yim and A. Amith, *Solid State Electron.* **15**:1141 (1972).
8. D. Y. Chung, T. Hogan, P. Brazis, M. Rocci-Lane, C. Kannewurf, M. Bastea, C. Uher, and M. G. Kanatzidis, *Science* **287**:1024 (2000).
9. C. B. Vining, *Proc. 11th Int. Conf. on Thermoelectrics* (Univ. Texas at Arlington, 1992), pp. 276–284.
10. J. C. Chen and Z. J. Yan, *J. Appl. Phys.* **79**:8823 (1996).
11. R. Venkatasubramanian, E. Silvola, T. Colpitts, and B. O'Quinn, *Nature* **413**:597 (2001).